HHS Public Access

Author manuscript

Anat Rec (Hoboken). Author manuscript; available in PMC 2016 December 01.

Published in final edited form as:

Anat Rec (Hoboken). 2015 December ; 298(12): 2018–2029. doi:10.1002/ar.23267.

Paradoxical Effects of Partial Leptin Deficiency on Bone in Growing Female Mice

Kenneth A. Philbrick[a], **Russell T. Turner**[a,b], **Adam J. Branscum**[c], **Carmen P. Wong**[a], and **Urszula T. Iwaniec**[a,b]

[a]Skeletal Biology Laboratory, School of Biological and Population Health Sciences, Oregon State University, Corvallis, OR 97331, USA

[b]Center for Healthy Aging Research, Oregon State University, Corvallis, OR 97331, USA

[c]Biostatistics Program, School of Biological and Population Health Sciences, Oregon State University, Corvallis, OR 97331, USA

Abstract

Morbidly obese, leptin-deficient *ob/ob* mice display low bone mass, mild osteoclast-rich osteopetrosis, and increased bone marrow adiposity. While partial leptin deficiency results in increased weight, the skeletal manifestations of partial leptin deficiency are less well defined. We therefore analyzed femora and lumbar vertebrae in growing (7-week-old) female C57BL/6 wildtype (WT) mice, partial leptin-deficient *ob/+* mice, and leptin-deficient *ob/ob* mice. The bones were evaluated by dual energy absorptiometry, microcomputed tomography and histomorphometry. As expected, *ob/+* mice were heavier, had more white adipose tissue, and lower serum leptin than WT mice, but were lighter and had less white adipose tissue than *ob/ob* mice. With a few exceptions, cancellous bone architecture, cell (osteoblast, osteoclast, and adipocyte), and dynamic measurements did not differ between WT and *ob/+* mice. In contrast, compared to WT and *ob/+* mice, *ob/ob* mice had lower cancellous bone volume fraction and higher bone marrow adiposity in the femur metaphysis, and higher cancellous bone volume fraction in lumbar vertebra. Paradoxically, *ob/+* mice had greater femoral bone volume than either WT or *ob/ob* mice. There was a positive correlation between body weight and femur volume in all three genotypes. However, the positive effect of weight on bone occurred with lower body weight in leptin-producing mice. The paradoxical differences in bone size among WT, *ob/+*, and *ob/ob* mice may be explained if leptin, in addition to stimulating bone growth and cancellous bone turnover, acts to lower the set-point at which increased body weight leads to a commensurate increase in bone size.

Keywords

ob/ob mice; *ob/+* mice; obesity; histomorphometry; microcomputed tomography

Corresponding author: Urszula T. Iwaniec, Ph.D., Skeletal Biology Laboratory, School of Biological and Population Health Sciences, Oregon State University, Corvallis, OR 97331, Tel: 541-737-9925, Fax: 541-737-6914, urszula.iwaniec@oregonstate.edu.

Disclosure Statement: The authors have nothing to disclose.

Introduction

Leptin, the protein product of the *ob* gene, is a pleotropic hormone produced primarily by adipocytes and has well-defined roles in regulation of appetite and energy metabolism (Ahima and Flier, 2000). Leptin levels in blood are positively associated with adipose tissue mass (Friedman and Halaas, 1998). The hormone crosses the blood brain barrier and acts at the hypothalamus to communicate the size of peripheral energy stores (Harris, 2013). Leptin deficiency due to inactivation of the leptin (*ob*) gene results in morbid obesity (Zhang et al., 1994; Campfield et al., 1995; Montague et al., 1997). Heterozygosity for the *ob* gene (*ob*/+) results in reduced leptin production by adipocytes and, in mice, leads to a compensatory increase in adipose tissue mass (Chung et al., 1998). Partial leptin deficiency in *ob*/+ mice is associated with several metabolic abnormalities, including glucose intolerance, and increased expression of lipogenic genes in the liver. Furthermore, *ob*/+ mice exhibit accentuated detrimental metabolic alterations when fed a high fat diet (Begriche et al., 2008).

Studies performed in leptin-deficient *ob/ob* mice demonstrate that the skeleton is a leptin target tissue. Specifically, leptin enhances postnatal bone growth and is essential for normal bone turnover. At the cellular level, leptin: 1) increases chondrocyte differentiation and matrix maturation during endochondral ossification, 2) increases osteoclast activity, and 3) increases osteoblast number and activity (Kishida et al., 2005; Handschin et al., 2007; Turner et al., 2013). In addition, leptin suppresses differentiation of mesenchymal stem cells to bone marrow adipocytes (Hess et al., 2005). As a consequence, mice with impaired leptin signaling (leptin-deficient *ob/ob* mice or leptin receptor-deficient *db/db* mice) display low bone mass, mild osteoclast-rich osteopetrosis, increased bone marrow adiposity, and overall poor bone material and mechanical properties (Hamrick et al., 2005; Ealey et al., 2006; Williams et al., 2011; Turner et al., 2013).

Total leptin deficiency is rare in humans (Friedman and Halaas, 1998). In contrast, partial leptin deficiency due to heterozygosity in the *ob* gene or polymorphisms in the 5′-untranslated region of the *ob* gene is more prevalent (Hager et al., 1998; Farooqi and O'Rahilly, 2004). Even more common are physiological (e.g., menopause) and pathological (e.g., type 1 diabetes) changes that alter levels of factors (e.g., sex steroids and insulin) known to regulate leptin secretion by adipocytes (Hardie et al., 1996; Barr et al., 1997; Casabiell et al., 1998; Brann et al., 1999; Lambrinoudaki et al., 2008). Although there is compelling evidence that leptin is required for normal bone growth, turnover, and biomechanical competence, it is not clear whether partial leptin deficiency affects the skeleton. To address this question, we evaluated: 1) bone mass, density, and architecture, 2) indices of bone growth and turnover, and 3) bone marrow adiposity in leptin-replete (+/+) wildtype (WT) mice, partial leptin-deficient heterozygous (*ob*/+) mice, and leptin-deficient homozygous (*ob/ob)* mice.

Materials and Methods

Experimental Design

Four-week-old colony littermate female C57BL/6 WT (+/+, n=10), *ob*/+ (n=8), and *ob/ob* (n=5) mice were purchased from Jackson Laboratory (Bar Harbor, Maine). Growing mice were used to lessen complications associated with chronic morbid obesity in *ob/ob* mice (Turner et al., 2014). The animals were maintained in accordance with the NIH Guide for the Care and the Use of Laboratory Animals, and the experimental protocol was approved by the Institutional Animal Care and Use Committee at Oregon State University. The mice were housed individually in a climate-controlled room (21°C, 38% humidity) on a 12 hr light/dark cycle, and fed standard rodent chow *ad libitum* (Teklad 8604, Harlen Laboratories, Indianapolis, IN). Food consumption and body weight were recorded weekly. The fluorochrome declomycin (20 mg/kg, Sigma, St. Louis, MO) was administered subcutaneously 9 days prior to necropsy and the fluorochrome calcein (20 mg/kg, Sigma, St. Louis, MO) was administered subcutaneously 4 days and 1 day prior to necropsy to label mineralizing bone. Mice were necropsied at 7 weeks (48 days) of age.

Tissue Collection

For tissue collection, mice were anesthetized with 2–3% isofluorane delivered in oxygen. Blood was collected via cardiac puncture and serum stored at −80°C for measurement of leptin and biochemical markers of bone turnover. Uteri and abdominal white adipose tissue were excised and weighed. Femora and 5^{th} lumbar vertebrae were collected, stored in 70% ethanol and analyzed using dual energy x-ray absorptiometry (DXA), microcomputed tomography (μCT), and histomorphometry.

Serum Chemistry

Serum leptin and carboxy-terminal collagen crosslinks (CTx) were measured by ELISA (Mouse Leptin Quantikine ELISA kit, R&D Systems, Minneapolis, MN and Mouse CTx ELISA kit, Life Sciences Advanced Technologies, Saint Petersburg, FL, respectively).

Dual Energy X-ray Absorptiometry

Total femur bone mineral content (BMC, g), area (cm^2), and bone mineral density (BMD, g/cm^2) were measured *ex vivo* using DXA (Piximus 2, Lunar Corp., Madison, WI).

Microcomputed Tomography

μCT was used for nondestructive 3-dimensional evaluation of bone length, volume and architecture (Bouxsein et al., 2010). Total femora and 5^{th} lumbar vertebrae were scanned in 70% ethanol using a Scanco μCT40 scanner (Scanco Medical AG, Basserdorf, Switzerland) at a voxel size of 12 x 12 x 12 μm (55 kV_p x-ray voltage, 145 μA intensity, and 200 ms integration time). Filtering parameters sigma and support were set to 0.8 and 1, respectively. Bone segmentation was conducted at a threshold of 245 (scale, 0–1000) determined empirically. Femur length was measured digitally in scout view (preliminary x-ray image) as the distance between the top of the femoral head and bottom of the medial condyle. Entire femora were evaluated for total femur bone volume followed by evaluation of cortical bone

in the femur diaphysis and cancellous bone in the distal femur metaphysis and epiphysis. Automated contouring was used to delineate cortical bone from non-bone. Following, all cortical slices were examined visually for evidence of cancellous struts originating from the endocortex (extremely rare at this site) and manually removed when present. For the femoral diaphysis, 20 consecutive slices (240 μm) of bone were evaluated 60% distal to the top of the femoral head and cross-sectional volume (cortical and marrow volume, mm^3), cortical volume (mm^3), marrow volume (mm^3), and cortical thickness (μm) were measured. Three-dimensional cortical volume measurements were converted to 2-dimensional area measurements (Bouxsein et al., 2010). Polar moment of inertia (I_{Polar}) was determined as a surrogate measure of bone strength in torsion. For the femoral metaphysis, 42 consecutive slices (504 μm) of cancellous bone, 45 consecutive slices (540 μm) proximal to the growth plate, were evaluated. The entire cancellous compartment (38 ± 1 slices, 456 ± 12 μm, mean ± SE) was assessed in the femoral epiphysis. Analysis of lumbar vertebra included the entire region of cancellous bone between the cranial and caudal growth plates (135 ± 1 slices, 1,620 ± 12 μm). Manual contouring was used to delineate cancellous from cortical bone in the femur metaphysis, femur epiphysis, and vertebral body. Direct cancellous bone measurements in the femur and lumbar vertebra included cancellous bone volume fraction (bone volume/tissue volume, %), connectivity density (mm^{-3}), trabecular thickness (μm), trabecular number (mm^{-1}), and trabecular spacing (μm).

Histomorphometry

The histological methods used here were described in detail (Iwaniec et al., 2008). In brief, following μCT evaluation, distal femora and 5^{th} lumbar vertebrae were dehydrated in a graded series of ethanol and xylene, and embedded undecalcified in modified methyl methacrylate. Longitudinal sections (4 μm thick) were cut with a vertical bed microtome (Leica 2065) and affixed to slides precoated with 1% gelatin solution. One section per specimen was left unstained and used for measurement of fluorochrome labels and one section per specimen was stained with toluidine blue (Sigma, St Louis, MO) and used for cell-based measurements. Longitudinal growth rate in the distal femur was determined as the distance between the hypertrophic zone undergoing calcification (calcein label) and the declomycin label front divided by the 8 day interlabel interval (μm/day). Total growth plate thickness (μm) was also measured, followed by individual measurement of the hypertrophic and proliferative zone thicknesses (μm). Cancellous bone was evaluated in the distal femur metaphysis and vertebral body. The region of interest in the distal femur metaphysis included area extending from 0.5 to 1.0 mm proximal to the growth plate and 0.25 mm from the cortical margins. The region of interest in the lumbar vertebra included the entire cancellous compartment between the cranial and caudal growth plates extending 0.25 mm from the growth plates and cortical margins. Fluorochrome-based measurements of cancellous bone formation included: 1) mineralizing perimeter (mineralizing perimeter/bone perimeter: cancellous bone perimeter covered with double plus half single label normalized to bone perimeter, %), 2) mineral apposition rate (the distance between two calcein markers that comprise a double label divided by the 3 day interlabel interval, μm/day), and 3) bone formation rate (bone formation rate/bone perimeter: calculated by multiplying mineralizing perimeter by mineral apposition rate normalized to bone perimeter, $\mu m^2/\mu m/y$). Cell-based measurements included osteoblast perimeter (osteoblast perimeter/bone perimeter, %),

osteoclast perimeter (osteoclast perimeter/bone perimeter, %), bone marrow adiposity (adipocyte area/tissue area, %), and adipocyte density (number/tissue area, #/mm^2). Osteoblasts were identified as cuboidal cells located immediately adjacent to a thin layer of osteoid in direct physical contact with bone. Osteoclasts were identified as multinucleated (two or more nuclei) cells in contact with the bone surface. Adipocytes were identified as large circular or oval-shaped cells bordered by a prominent cell membrane and lacking cytoplasmic staining due to alcohol extraction of intracellular lipids during processing. This method has been previously validated by fat extraction and analysis (Menagh et al., 2010). All data were collected using the OsteoMeasure System (OsteoMetrics, Inc., Atlanta, GA) and are reported using standard nomenclature (Dempster et al., 2013).

Statistics

Mean responses of individual variables were compared between WT, *ob/+*, and *ob/ob* groups using separate one-way analyses of variance (ANOVA). A modified F test was used when the assumption of equal variance was violated, with Welch's two-sample t-test used for pairwise comparisons (Welch, 1951). The Kruskal-Wallis nonparametric test was used when only the normality assumption was violated, in which case the Wilcoxon-Mann-Whitney test was used for pairwise comparisons. Bone volume was the dependent variable in a multiple linear regression analysis that included body weight, group (WT, *ob/+*, *ob/ob*), and their interaction as independent variables to test for different correlations between body weight and femoral and vertebral total bone volume among groups. A Pearson correlation between body weight and total bone volume was calculated among groups. The required conditions for valid use of ANOVA and linear regression were assessed using Levene's test for homogeneity of variance, plots of residuals versus fitted values, normal quantile plots, and the Anderson-Darling test of normality. The Benjamini and Hochberg (Benjamini and Hochberg, 1995) method for maintaining the false discovery rate at 5% was used to adjust for multiple comparisons. Data analysis was performed using R version 2.12 (Team, 2010). Differences were considered significant at $P < 0.05$. All data are expressed as mean ± SE.

Results

The effects of genotype on body weight, abdominal white adipose tissue weight, food consumption, uterine weight, serum leptin, and serum CTx are shown in Figure 1 (A–F). Seven-week-old *ob/+* mice had greater body weight (A) and abdominal white adipose tissue weight (B), and consumed more food (C) than WT mice. Significant differences in uterine weight (D) and serum CTx (F) were not detected between *ob/+* and WT mice. Serum leptin (E) was lower in *ob/+* mice than in WT mice. Body weight, abdominal white adipose tissue weight, and food consumption were higher, and uterine weight and serum Ctx were lower in *ob/ob* mice compared to either WT or *ob/+* mice. As expected, leptin was not detected in serum of *ob/ob* mice.

Dual Energy X-ray Absorptiometry

The effects of genotype on femur BMC, area, and BMD are shown in Figure 2 (A–C). *ob/+* mice had higher femur BMC (A), area (B), and tended ($P<0.1$) to have higher BMD (C) than

WT mice. Femur BMC and BMD were lower in *ob/ob* mice compared to either WT or *ob/+* mice.

Microcomputed Tomography

The effects of genotype on femur length, total femur bone volume, and cortical bone architecture in the femur diaphysis are shown in Figure 2 (D–K). *ob/+* mice had longer femora (D), greater total femur bone volume (E), and greater total femur bone volume to length ratio (F) than WT mice. Furthermore, *ob/+* mice had greater diaphyseal femur cross-sectional area (G), cortical bone area (H), marrow area (I), and polar moment of inertia (K) than WT mice. Femur length, total femur bone volume, and total femur bone volume to length ratio were lower in *ob/ob* mice compared to *ob/+* mice. There was also a tendency ($P < 0.1$) for femur length to be lower in *ob/ob* mice compared to WT mice. Diaphyseal femur cross-sectional area, marrow area, and polar moment of inertia were greater in *ob/ob* mice compared to WT mice. Significant differences in cortical thickness (J) were not detected among genotypes.

The relationship between body weight and total femur bone volume, an index of bone size, is shown for each genotype in Figure 3A. A positive correlation between body weight and total femur bone volume was observed in WT mice (Pearson $r = 0.75$), *ob/+* mice (Pearson $r = 0.91$), and *ob/ob* mice (Pearson $r = 0.96$). Significant differences in regression slopes were not detected among the 3 genotypes. Adjusted for body weight, there was no evidence of statistical difference in mean femur bone volume between WT and ob/+ mice (multiple linear regression, $P = 0.89$).

The effects of genotype on cancellous bone in distal femur metaphysis and distal femur epiphysis are shown in Table 1. Cancellous bone volume fraction in distal femur metaphysis tended ($P<0.1$) to be lower in *ob/+* mice compared to WT mice. However, significant differences in cancellous bone architecture were not detected between the two genotypes. In contrast, cancellous bone volume fraction, connectivity density, and trabecular number were lower and trabecular spacing tended ($P<0.1$) to be higher in *ob/ob* mice compared to WT mice. Significant differences in trabecular thickness were not detected among genotypes.

Significant differences in cancellous bone volume fraction, connectivity density, and trabecular thickness were not detected between *ob/+* and WT mice in distal femur epiphysis. However, trabecular number was lower and trabecular spacing was higher in *ob/+* mice compared to WT mice. Connectivity density and trabecular number were higher and trabecular thickness and spacing were lower in *ob/ob* compared to either WT or *ob/+* mice.

The effects of genotype on total lumbar vertebra bone volume and on cancellous bone in the lumbar vertebral body are shown in Table 2. *ob/+* mice had greater total vertebral bone volume than either WT or *ob/ob* mice. Significant differences in vertebral cancellous bone volume fraction and architecture were not detected between WT and *ob/+* mice. In contrast, cancellous bone volume fraction, connectivity density, and trabecular number were higher and trabecular spacing was lower in *ob/ob* mice than in either WT or *ob/+* mice. Significant differences in trabecular thickness were not detected among genotypes.

The relationship between body weight and total vertebra bone volume in each genotype is shown in Figure 3B. A positive correlation between body weight and total vertebra bone volume was observed in WT mice (Pearson r = 0.83). A significant correlation was not detected in *ob/+* mice (Pearson r = 0.44) or *ob/ob* mice (Pearson r = 0.74).

Histomorphometry

The effects of genotype on longitudinal growth rate, and on total growth plate, hypertrophic zone, and proliferative zone thicknesses in distal femur metaphysis are shown in Figure 4 (A–D). Significant differences in longitudinal growth rate (A), growth plate thickness (B), and proliferative zone thickness (C) were not detected between *ob/+* and WT mice. Longitudinal growth rate and growth plate thickness were lower in *ob/ob* mice than in either WT or *ob/+* mice while proliferative zone thickness was lower in *ob/ob* mice than in WT mice. Significant differences in hypertrophic zone thickness were not detected among genotypes.

The effects of genotype on mineralizing perimeter, mineral apposition rate, bone formation rate, osteoblast perimeter, osteoclast perimeter, bone marrow adiposity, and bone marrow adipocyte density in distal femur metaphysis are shown in Figure 5 (A–J). Significant differences in mineralizing perimeter (A), mineral apposition rate (B), bone formation rate (C), and osteoblast perimeter (D) were not detected between WT and *ob/+* mice while bone marrow adiposity (F) and adipocyte density (G) tended ($P<0.1$) to be lower in *ob/+* mice than in WT mice. In contrast, mineralizing perimeter, mineral apposition rate, and bone formation rate were lower while bone marrow adiposity and adipocyte density were higher in *ob/ob* mice compared to either WT or *ob/+* mice. The more extensive bone marrow adiposity in *ob/ob* mice compared to WT and *ob/+* mice can be readily appreciated in Figure 5 H–J. Significant differences in osteoclast perimeter (E) were not detected among genotypes.

The effects of genotype on mineralizing perimeter, mineral apposition rate, bone formation rate, osteoblast perimeter, and osteoclast perimeter in lumbar vertebra are shown in Figure 6 (A–E). Significant differences in mineralizing perimeter (A), bone formation rate (C), and osteoblast perimeter (D) were not detected between WT and *ob/+* mice, while mineral apposition rate (B) was lower in *ob/+* mice than in WT mice. Mineralizing perimeter and osteoblast perimeter were lower in *ob/ob* mice compared to either WT or *ob/+* mice, while bone formation rate was lower in *ob/ob* mice than in WT mice and tended ($P<0.1$) to be lower in *ob/ob* mice than in *ob/+* mice. Significant differences in osteoclast perimeter (E) were not detected among genotypes. Negligible bone marrow adiposity was observed in vertebra of the three genotypes (data not shown).

Discussion

Partial leptin-deficient heterozygous *ob/+* mice were heavier, had increased abdominal white adipose tissue, and lower serum leptin levels compared to WT mice. In addition, *ob/+* mice had larger femora and vertebrae than WT mice. Longitudinal growth rate, cancellous bone volume fraction and architecture, cell and dynamic measurements of cancellous bone formation, and cell and serum indices of bone resorption generally did not differ between

WT and *ob/+* mice. Exceptions included a tendency (P <0.1) for decreased bone volume fraction in distal femur metaphysis, decreased trabecular number and increased trabecular spacing in distal femur epiphysis, and decreased mineral apposition rate in lumbar vertebra. Lack of differences in longitudinal growth rate between WT and ob/+ mice suggest that greater femur length in *ob/+* mice was due to a transient increase in longitudinal growth rate prior to 7 weeks of age. As expected, leptin-deficient *ob/ob* mice were heavier, had more abdominal white adipose tissue and were hyperphagic compared to WT and *ob/+* mice. In addition, the majority of cancellous bone parameters in *ob/ob* mice differed from WT and *ob/+* mice.

ob/ob mice are infertile and are generated by breeding *ob/+* males and *ob/+* females (Chehab et al., 1996). *ob/ob* mice can be distinguished from WT and *ob/+* mice by time of weaning because of increased body weight. Ungenotyped lean littermate controls are genetically ambiguous ob/? and consist of a mixture of WT and *ob/+* offspring. The present study demonstrates that the skeletal phenotype of WT and *ob/+* mice are not identical, indicating that studies investigating the specific effects of leptin on bone metabolism should take into account the distinct skeletal phenotype of *ob/+* mice.

The precise effects of leptin deficiency on bone mass, mineral density, and architecture vary with age, bone, and bone compartment (Steppan et al., 2000; Hamrick et al., 2005; Williams et al., 2011). Leptin acts on growth plate cartilage cells, osteoblasts, and osteoclasts to enhance their number and/or activity (Steppan et al., 2000; Kalra et al., 2009; Bartell et al., 2011). A combination of reduced longitudinal bone growth and reduced bone turnover is the likely explanation for the “mosaic” skeletal phenotype reported in *ob/ob* mice (Turner et al., 2013). The abnormal skeletal architecture of femur (e.g., decreased length) and vertebra (e.g., increased cancellous bone volume fraction) observed in rapidly growing female *ob/ob* mice in the present study is consistent with this interpretation.

The skeletal phenotype of *ob/+* mice has not been described in detail. Ducy et al. (Ducy et al., 2000) reported that *ob/+* mice of unspecified gender and serum leptin levels were lean and exhibited increased cancellous bone volume fraction (measured at 3 months of age) and increased bone formation rate (measured at 1 month of age) in lumbar vertebra, leading the authors to conclude that the heterozygous mutants have a high cancellous bone mass phenotype associated with increased bone formation. In the present study, vertebral cancellous bone volume fraction and bone formation rate did not differ between 7-week-old WT and *ob/+* mice. In addition, significant differences in cancellous bone volume fraction and bone formation rate were not detected in the distal femur metaphysis, although there was a tendency (P<0.1) for metaphyseal cancellous bone volume fraction to be lower in the *ob/+* mice compared to WT mice. The reason for the discrepancy in the results regarding body weight and vertebral cancellous bone volume parameters reported by Ducy et al. and the current study is not self-evident.

The present study extends previous work by evaluating the cortical bone phenotype in growing female *ob/+* mice. Total femur bone mass and length and midshaft femur cross-sectional area, cortical area, and marrow area were increased in the heterozygous mice compared to WT mice. Consistent with other reports (Chung et al., 1998), *ob/+* mice

exhibited increased body weight and increased adipose tissue weight but decreased blood leptin levels compared to WT mice. Taken together, our findings suggest that partial leptin deficiency leads to compartment-specific changes in bone architecture that, with the exceptions noted above, are not intermediate between WT and *ob/ob* mice.

We have previously reported a positive association between body weight and bone mass in WT mice (Iwaniec et al., 2009). The results of the present study suggest that increased weight is sufficient to account for the difference in total femur bone volume between WT and *ob/+* mice. Although there was a positive association between body weight and total femur bone volume in *ob/ob* mice in this and a prior study (Iwaniec et al., 2009), our results suggest that the presence of leptin increases sensitivity of the skeletal response to increased body weight. In this regard, there is evidence that leptin modulates mechanosensitivity of the skeleton (Baek and Bloomfield, 2009; Kapur et al., 2010). However, we cannot rule out the possibility of other mechanisms. For example, *ob/ob* mice are hypogonadal and estrogen has been shown to increase the mechanosensitivity of the skeleton by changing the set-point at which bone responds to mechanical load (Luo et al., 2000). Alternatively, it is possible that reduced physical activity or one or more adipokines antagonize the positive effect of weight gain on bone mass in *ob/ob* mice. Finally, bone and muscle size is associated with serum IGF-I levels, which are reduced in *ob/ob* mice and increased following leptin administration (Bartell et al., 2011). As a consequence, differences in muscle mass, strength or physical activity levels may have contributed to the genotype-associated differences in bone size (Bartell et al., 2011) and future studies are required to tease out specific potential effects and establish the precise mechanisms of action.

Body weight would be expected to subject the vertebra to less mechanical loading than femur. Nevertheless, a positive relationship between body weight and vertebral bone volume was found in WT mice. Although this relationship was not significant for *ob/ob* mice over the weight range evaluated, there was a clear separation in bone volume versus body weight between leptin-producing and morbidly obese, leptin-deficient *ob/ob* mice.

Whereas bone mass is also positively associated with body mass in humans (Wildner et al., 2003), this association is less apparent in the morbidly obese (Bredella et al., 2011; Yoo et al., 2012). Leptin resistance is thought to contribute to development of morbid obesity (Jung and Kim, 2013). We speculate that development of leptin resistance in obese individuals may play a causal role for impaired skeletal adaptation to greatly increased body weight.

Leptin is produced primarily by adipocytes and circulates in levels proportional to total body adiposity (Zhang et al., 1994; Maffei et al., 1995; Considine et al., 1996). However, the production and secretion of leptin by adipocytes is regulated by a variety of systemic factors, including insulin, thyroid hormone, prolactin, steroid hormones, 1,25-dihydroxyvitamin D, pro-inflammatory cytokines and short-chained fatty acids (Kristensen et al., 1999; Scriba et al., 2000; Kalsbeek et al., 2001; Ling and Billig, 2001; Bruun et al., 2002; Garcia et al., 2002; Fain et al., 2003; Menendez et al., 2003; Abelenda and Puerta, 2004; Xiong et al., 2004; Brandebourg et al., 2007; Szkudelski, 2007; Soliman et al., 2011; Ciardi et al., 2012; Kong et al., 2013). Thus, changes in blood leptin levels may contribute to the mechanisms by which a variety of factors regulate bone metabolism. Administration of leptin has

dramatic effects on bone growth and turnover in leptin-deficient *ob/ob* mice. On the other hand, changes in leptin levels induced by either mild caloric restriction or excess have no effect on bone turnover in skeletally mature rats (Turner and Iwaniec, 2010). Similarly, increasing leptin levels in the hypothalamus of rats by gene therapy suppressed weight gain and lowered serum leptin levels without impacting bone turnover (Iwaniec et al., 2011). Taken together, these findings suggest that many of the important actions of leptin on bone metabolism are achieved at relatively low circulating levels of the hormone.

A notable characteristic of the skeleton of morbidly obese *ob/ob* mice is the excessive bone marrow adiposity which is reversed following leptin treatment (Bartell et al., 2011). Osteoblasts and adipocytes are derived from a common mesenchymal stromal cell (Rosen and Bouxsein, 2006a; Rosen and Bouxsein, 2006b). It is possible that leptin enhances bone formation, at least in part, by influencing the fate of differentiating mesenchymal stromal cells to promote osteoblast differentiation (Thomas et al., 1999a; Thomas et al., 1999b). However, in the present study performed in young mice, high levels of fat infiltration into bone marrow were only noted in the femur. In contrast, osteoblast-lined bone perimeter was reduced in lumbar vertebra in this and prior studies (Turner et al., 2013). Thus, the decreased bone formation in *ob/ob* mice is not universally associated with increased bone marrow adiposity.

ob/ob mice become morbidly obese and develop type 2 diabetes. We have recently reported that morbid obesity impacts the skeletal phenotype of *ob/ob* mice (Turner et al., 2014). The current experiment was designed to identify skeletal abnormalities present during growth in leptin-deficient *ob/ob* mice and partially leptin-deficient *ob/+* mice. While we have not performed a comparison study in adult WT, *ob/+*, and *ob/ob* mice, we have conducted detailed μCT analysis of the skeletal phenotype of adult (4-month-old) female leptin receptor-deficient *db/db*, partially leptin receptor-deficient *db/+*, and WT mice (data not shown). *ob/+* mice are partially leptin signaling deficient because they have a reduced capacity to generate leptin. In contrast, *db/+* mice are partially leptin signaling deficient because of their reduced capacity to generate the signaling form of the leptin receptor. The data suggest that the skeletal differences associated with partial leptin deficiency observed in the young *ob/ob* mice are also observed in the adult partial leptin receptor-deficient db/+ mice, indicating that the higher cortical bone mass in the growing *ob/+* mice is likely to be preserved into adulthood.

In conclusion, heterozygote *ob*/+ mice adapt to partial leptin deficiency by increasing adipose tissue mass. An increase in body weight in partial leptin-deficient *ob/+* mice is associated with a commensurate increase in bone size. A similar relationship in leptin-deficient *ob/ob* mice at a much higher body weight suggests that leptin acts, directly or indirectly, to increase the sensitivity of the skeleton to adapt to increased weight.

Acknowledgments

Grant Sponsors: NIH, AR 060913: NASA, NNX12AL24: and USDA, 38420-17804.

Literature Cited

Abelenda M, Puerta M. Leptin release is decreased in white adipocytes isolated from progesterone-treated rats. Endocrine research. 2004; 30:335–342. [PubMed: 15554349]

Ahima RS, Flier JS. Leptin. Annual review of physiology. 2000; 62:413–437.

Baek K, Bloomfield SA. Beta-adrenergic blockade and leptin replacement effectively mitigate disuse bone loss. Journal of bone and mineral research. 2009; 24:792–799. [PubMed: 19113907]

Barr VA, Malide D, Zarnowski MJ, Taylor SI, Cushman SW. Insulin stimulates both leptin secretion and production by rat white adipose tissue. Endocrinology. 1997; 138:4463–4472. [PubMed: 9322964]

Bartell SM, Rayalam S, Ambati S, Gaddam DR, Hartzell DL, Hamrick M, She JX, Della-Fera MA, Baile CA. Central (ICV) leptin injection increases bone formation, bone mineral density, muscle mass, serum IGF-1, and the expression of osteogenic genes in leptin-deficient ob/ob mice. Journal of bone and mineral research. 2011; 26:1710–1720. [PubMed: 21520275]

Begriche K, Letteron P, Abbey-Toby A, Vadrot N, Robin MA, Bado A, Pessayre D, Fromenty B. Partial leptin deficiency favors diet-induced obesity and related metabolic disorders in mice. American journal of physiology Endocrinology and metabolism. 2008; 294:E939–951. [PubMed: 18349116]

Benjamini Y, Hochberg Y. Controlling the false discovery rate: a practical and powerful approach to multiple testing. Journal of the Royal Statistical Society Series B. 1995; 57:289–300.

Bouxsein ML, Boyd SK, Christiansen BA, Guldberg RE, Jepsen KJ, Muller R. Guidelines for assessment of bone microstructure in rodents using micro-computed tomography. Journal of bone and mineral research. 2010; 25:1468–1486. [PubMed: 20533309]

Brandebourg TD, Bown JL, Ben-Jonathan N. Prolactin upregulates its receptors and inhibits lipolysis and leptin release in male rat adipose tissue. Biochemical and biophysical research communications. 2007; 357:408–413. [PubMed: 17433256]

Brann DW, De Sevilla L, Zamorano PL, Mahesh VB. Regulation of leptin gene expression and secretion by steroid hormones. Steroids. 1999; 64:659–663. [PubMed: 10503725]

Bredella MA, Torriani M, Ghomi RH, Thomas BJ, Brick DJ, Gerweck AV, Harrington LM, Breggia A, Rosen CJ, Miller KK. Determinants of bone mineral density in obese premenopausal women. Bone. 2011; 48:748–754. [PubMed: 21195217]

Bruun JM, Pedersen SB, Kristensen K, Richelsen B. Effects of pro-inflammatory cytokines and chemokines on leptin production in human adipose tissue in vitro. Molecular and cellular endocrinology. 2002; 190:91–99. [PubMed: 11997182]

Campfield LA, Smith FJ, Guisez Y, Devos R, Burn P. Recombinant mouse OB protein: evidence for a peripheral signal linking adiposity and central neural networks. Science. 1995; 269:546–549. [PubMed: 7624778]

Casabiell X, Pineiro V, Peino R, Lage M, Camina J, Gallego R, Vallejo LG, Dieguez C, Casanueva FF. Gender differences in both spontaneous and stimulated leptin secretion by human omental adipose tissue in vitro: dexamethasone and estradiol stimulate leptin release in women, but not in men. The Journal of clinical endocrinology and metabolism. 1998; 83:2149–2155. [PubMed: 9626154]

Chehab FF, Lim ME, Lu R. Correction of the sterility defect in homozygous obese female mice by treatment with the human recombinant leptin. Nature genetics. 1996; 12:318–320. [PubMed: 8589726]

Chung WK, Belfi K, Chua M, Wiley J, Mackintosh R, Nicolson M, Boozer CN, Leibel RL. Heterozygosity for Lep(ob) or Lep(rdb) affects body composition and leptin homeostasis in adult mice. The American journal of physiology. 1998; 274:R985–990. [PubMed: 9575960]

Ciardi C, Jenny M, Tschoner A, Ueberall F, Patsch J, Pedrini M, Ebenbichler C, Fuchs D. Food additives such as sodium sulphite, sodium benzoate and curcumin inhibit leptin release in lipopolysaccharide-treated murine adipocytes in vitro. The British journal of nutrition. 2012; 107:826–833. [PubMed: 21801469]

Considine RV, Sinha MK, Heiman ML, Kriauciunas A, Stephens TW, Nyce MR, Ohannesian JP, Marco CC, McKee LJ, Bauer TL, et al. Serum immunoreactive-leptin concentrations in normal-

weight and obese humans. The New England journal of medicine. 1996; 334:292–295. [PubMed: 8532024]

Dempster DW, Compston JE, Drezner MK, Glorieux FH, Kanis JA, Malluche H, Meunier PJ, Ott SM, Recker RR, Parfitt AM. Standardized nomenclature, symbols, and units for bone histomorphometry: a 2012 update of the report of the ASBMR Histomorphometry Nomenclature Committee. Journal of bone and mineral research. 2013; 28:2–17. [PubMed: 23197339]

Ducy P, Amling M, Takeda S, Priemel M, Schilling AF, Beil FT, Shen J, Vinson C, Rueger JM, Karsenty G. Leptin inhibits bone formation through a hypothalamic relay: a central control of bone mass. Cell. 2000; 100:197–207. [PubMed: 10660043]

Ealey KN, Fonseca D, Archer MC, Ward WE. Bone abnormalities in adolescent leptin-deficient mice. Regulatory peptides. 2006; 136:9–13. [PubMed: 16764953]

Fain JN, Kanu A, Bahouth SW, Cowan GS, Lloyd Hiler M. Inhibition of leptin release by atrial natriuretic peptide (ANP) in human adipocytes. Biochemical pharmacology. 2003; 65:1883–1888. [PubMed: 12781340]

Farooqi IS, O'Rahilly S. Monogenic human obesity syndromes. Recent progress in hormone research. 2004; 59:409–424. [PubMed: 14749512]

Friedman JM, Halaas JL. Leptin and the regulation of body weight in mammals. Nature. 1998; 395:763–770. [PubMed: 9796811]

Garcia MR, Amstalden M, Williams SW, Stanko RL, Morrison CD, Keisler DH, Nizielski SE, Williams GL. Serum leptin and its adipose gene expression during pubertal development, the estrous cycle, and different seasons in cattle. Journal of animal science. 2002; 80:2158–2167. [PubMed: 12211386]

Hager J, Clement K, Francke S, Dina C, Raison J, Lahlou N, Rich N, Pelloux V, Basdevant A, Guy-Grand B, North M, Froguel P. A polymorphism in the 5′ untranslated region of the human ob gene is associated with low leptin levels. International journal of obesity and related metabolic disorders. 1998; 22:200–205. [PubMed: 9539186]

Hamrick MW, Della-Fera MA, Choi YH, Pennington C, Hartzell D, Baile CA. Leptin treatment induces loss of bone marrow adipocytes and increases bone formation in leptin-deficient ob/ob mice. Journal of bone and mineral research. 2005; 20:994–1001. [PubMed: 15883640]

Handschin AE, Trentz OA, Hemmi S, Wedler V, Trentz O, Giovanoli P, Wanner GA. Leptin increases extracellular matrix mineralization of human osteoblasts from heterotopic ossification and normal bone. Annals of plastic surgery. 2007; 59:329–333. [PubMed: 17721225]

Hardie LJ, Guilhot N, Trayhurn P. Regulation of leptin production in cultured mature white adipocytes. Hormone and metabolic research = Hormon- und Stoffwechselforschung = Hormones et metabolisme. 1996; 28:685–689. [PubMed: 9013742]

Harris RB. Is leptin the parabiotic "satiety" factor? Past and present interpretations. Appetite. 2013; 61:111–118. [PubMed: 22889986]

Hess R, Pino AM, Rios S, Fernandez M, Rodriguez JP. High affinity leptin receptors are present in human mesenchymal stem cells (MSCs) derived from control and osteoporotic donors. Journal of cellular biochemistry. 2005; 94:50–57. [PubMed: 15517602]

Iwaniec UT, Boghossian S, Trevisiol CH, Wronski TJ, Turner RT, Kalra SP. Hypothalamic leptin gene therapy prevents weight gain without long-term detrimental effects on bone in growing and skeletally mature female rats. Journal of bone and mineral research. 2011; 26:1506–1516. [PubMed: 21328617]

Iwaniec UT, Dube MG, Boghossian S, Song H, Helferich WG, Turner RT, Kalra SP. Body mass influences cortical bone mass independent of leptin signaling. Bone. 2009; 44:404–412. [PubMed: 19095090]

Iwaniec UT, Wronski TJ, Turner RT. Histological analysis of bone. Methods in molecular biology. 2008; 447:325–341. [PubMed: 18369927]

Jung CH, Kim MS. Molecular mechanisms of central leptin resistance in obesity. Archives of pharmacal research. 2013; 36:201–207. [PubMed: 23359004]

Kalra SP, Dube MG, Iwaniec UT. Leptin increases osteoblast-specific osteocalcin release through a hypothalamic relay. Peptides. 2009; 30:967–973. [PubMed: 19428775]

Kalsbeek A, Fliers E, Romijn JA, La Fleur SE, Wortel J, Bakker O, Endert E, Buijs RM. The suprachiasmatic nucleus generates the diurnal changes in plasma leptin levels. Endocrinology. 2001; 142:2677–2685. [PubMed: 11356719]

Kapur S, Amoui M, Kesavan C, Wang X, Mohan S, Baylink DJ, Lau KH. Leptin receptor (Lepr) is a negative modulator of bone mechanosensitivity and genetic variations in Lepr may contribute to the differential osteogenic response to mechanical stimulation in the C57BL/6J and C3H/HeJ pair of mouse strains. The Journal of biological chemistry. 2010; 285:37607–37618. [PubMed: 20851886]

Kishida Y, Hirao M, Tamai N, Nampei A, Fujimoto T, Nakase T, Shimizu N, Yoshikawa H, Myoui A. Leptin regulates chondrocyte differentiation and matrix maturation during endochondral ossification. Bone. 2005; 37:607–621. [PubMed: 16039170]

Kong J, Chen Y, Zhu G, Zhao Q, Li YC. 1,25-Dihydroxyvitamin D3 upregulates leptin expression in mouse adipose tissue. The Journal of endocrinology. 2013; 216:265–271. [PubMed: 23160964]

Kristensen K, Pedersen SB, Langdahl BL, Richelsen B. Regulation of leptin by thyroid hormone in humans: studies in vivo and in vitro. Metabolism: clinical and experimental. 1999; 48:1603–1607. [PubMed: 10599995]

Lambrinoudaki IV, Christodoulakos GE, Economou EV, Vlachou SA, Panoulis CP, Alexandrou AP, Kouskouni EE, Creatsas GC. Circulating leptin and ghrelin are differentially influenced by estrogen/progestin therapy and raloxifene. Maturitas. 2008; 59:62–71. [PubMed: 18164562]

Ling C, Billig H. PRL receptor-mediated effects in female mouse adipocytes: PRL induces suppressors of cytokine signaling expression and suppresses insulin-induced leptin production in adipocytes in vitro. Endocrinology. 2001; 142:4880–4890. [PubMed: 11606456]

Luo ZP, Zhang L, Turner RT, An KN. Effects of mechanical stress/strain and estrogen on cancellous bone structure predicted by fuzzy decision. IEEE transactions on bio-medical engineering. 2000; 47:344–351. [PubMed: 10743776]

Maffei M, Halaas J, Ravussin E, Pratley RE, Lee GH, Zhang Y, Fei H, Kim S, Lallone R, Ranganathan S, et al. Leptin levels in human and rodent: measurement of plasma leptin and ob RNA in obese and weight-reduced subjects. Nature medicine. 1995; 1:1155–1161.

Menagh PJ, Turner RT, Jump DB, Wong CP, Lowry MB, Yakar S, Rosen CJ, Iwaniec UT. Growth hormone regulates the balance between bone formation and bone marrow adiposity. Journal of bone and mineral research : the official journal of the American Society for Bone and Mineral Research. 2010; 25:757–768.

Menendez C, Baldelli R, Camina JP, Escudero B, Peino R, Dieguez C, Casanueva FF. TSH stimulates leptin secretion by a direct effect on adipocytes. The Journal of endocrinology. 2003; 176:7–12. [PubMed: 12525244]

Montague CT, Farooqi IS, Whitehead JP, Soos MA, Rau H, Wareham NJ, Sewter CP, Digby JE, Mohammed SN, Hurst JA, Cheetham CH, Earley AR, Barnett AH, Prins JB, O'Rahilly S. Congenital leptin deficiency is associated with severe early-onset obesity in humans. Nature. 1997; 387:903–908. [PubMed: 9202122]

Rosen CJ, Bouxsein ML. Mechanisms of disease: is osteoporosis the obesity of bone? Nature clinical practice Rheumatology. 2006a; 2:35–43.

Rosen CJ, Bouxsein ML. Mechanisms of disease: is osteoporosis the obesity of bone? Nature clinical practice Rheumatology. 2006b; 2:35–43.

Scriba D, Aprath-Husmann I, Blum WF, Hauner H. Catecholamines suppress leptin release from in vitro differentiated subcutaneous human adipocytes in primary culture via beta1- and beta2-adrenergic receptors. European journal of endocrinology / European Federation of Endocrine Societies. 2000; 143:439–445. [PubMed: 11022189]

Soliman MM, Ahmed MM, Salah-Eldin AE, Abdel-Aal AA. Butyrate regulates leptin expression through different signaling pathways in adipocytes. Journal of veterinary science. 2011; 12:319–323. [PubMed: 22122897]

Steppan CM, Crawford DT, Chidsey-Frink KL, Ke H, Swick AG. Leptin is a potent stimulator of bone growth in ob/ob mice. Regulatory peptides. 2000; 92:73–78. [PubMed: 11024568]

Szkudelski T. Intracellular mediators in regulation of leptin secretion from adipocytes. Physiological research / Academia Scientiarum Bohemoslovaca. 2007; 56:503–512. [PubMed: 17184148]

Team RDC. A language and environment for statistical computing. Vienna, Austria: R Foundation for Statistical Computing; 2010.

Thomas T, Gori F, Khosla S, Jensen MD, Burguera B, Riggs BL. Leptin acts on human marrow stromal cells to enhance differentiation to osteoblasts and to inhibit differentiation to adipocytes. Endocrinology. 1999a; 140:1630–1638. [PubMed: 10098497]

Thomas T, Gori F, Khosla S, Jensen MD, Burguera B, Riggs BL. Leptin acts on human marrow stromal cells to enhance differentiation to osteoblasts and to inhibit differentiation to adipocytes. Endocrinology. 1999b; 140:1630–1638. [PubMed: 10098497]

Turner RT, Iwaniec UT. Moderate weight gain does not influence bone metabolism in skeletally mature female rats. Bone. 2010; 47:631–635. [PubMed: 20601291]

Turner RT, Kalra SP, Wong CP, Philbrick KA, Lindenmaier LB, Boghossian S, Iwaniec UT. Peripheral leptin regulates bone formation. Journal of bone and mineral research. 2013; 28:22–34. [PubMed: 22887758]

Turner RT, Philbrick KA, Wong CP, Olson DA, Branscum AJ, Iwaniec UT. Morbid obesity attenuates the skeletal abnormalities associated with leptin deficiency in mice. The Journal of endocrinology. 2014; 223:M1–15. [PubMed: 24990938]

Welch BL. On comparison of several mean values: an alternative approach. Biometrika. 1951; 38:330–336.

Wildner M, Peters A, Raghuvanshi VS, Hohnloser J, Siebert U. Superiority of age and weight as variables in predicting osteoporosis in postmenopausal white women. Osteoporosis international. 2003; 14:950–956. [PubMed: 13680102]

Williams GA, Callon KE, Watson M, Costa JL, Ding Y, Dickinson M, Wang Y, Naot D, Reid IR, Cornish J. Skeletal phenotype of the leptin receptor-deficient db/db mouse. Journal of bone and mineral research. 2011; 26:1698–1709. [PubMed: 21328476]

Xiong Y, Miyamoto N, Shibata K, Valasek MA, Motoike T, Kedzierski RM, Yanagisawa M. Short-chain fatty acids stimulate leptin production in adipocytes through the G protein-coupled receptor GPR41. Proceedings of the National Academy of Sciences of the United States of America. 2004; 101:1045–1050. [PubMed: 14722361]

Yoo HJ, Park MS, Yang SJ, Kim TN, Lim KI, Kang HJ, Song W, Baik SH, Choi DS, Choi KM. The differential relationship between fat mass and bone mineral density by gender and menopausal status. Journal of bone and mineral metabolism. 2012; 30:47–53. [PubMed: 21644057]

Zhang Y, Proenca R, Maffei M, Barone M, Leopold L, Friedman JM. Positional cloning of the mouse obese gene and its human homologue. Nature. 1994; 372:425–432. [PubMed: 7984236]

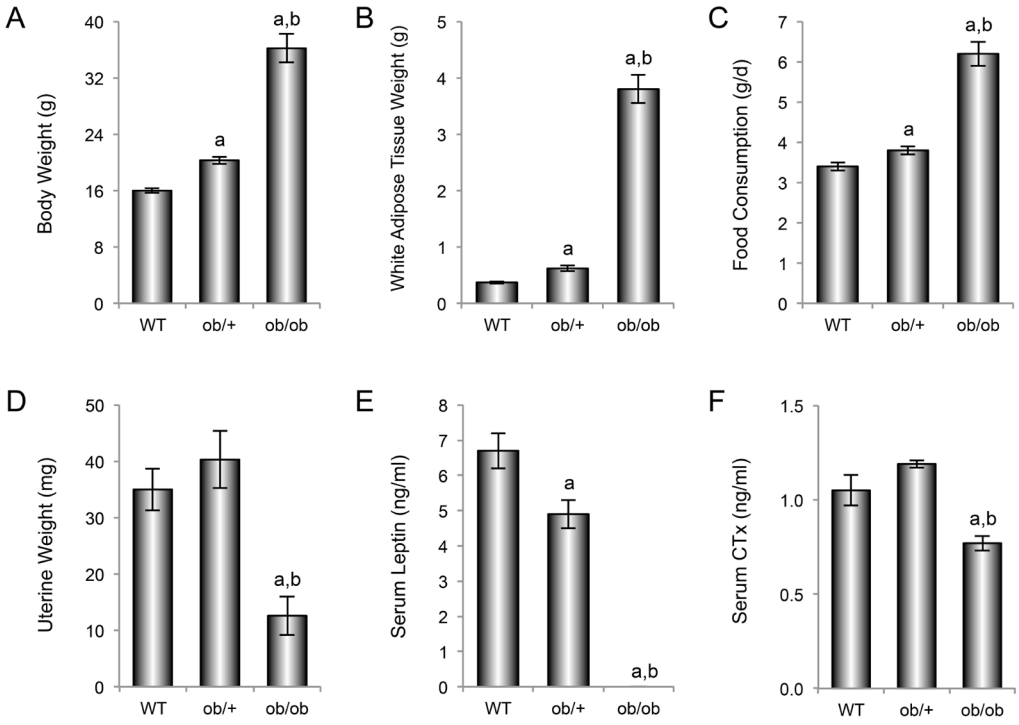

Figure 1.

Effects of genotype on body weight (A), abdominal white adipose tissue weight (B), food consumption (C), uterine weight (D), serum leptin (E), and serum CTx (F) in 7-week-old female WT, *ob/+*, and *ob/ob* mice. Data are mean ± SE. [a]Different from WT, $P < 0.05$; [b]Different from *ob/+*, $P < 0.05$.

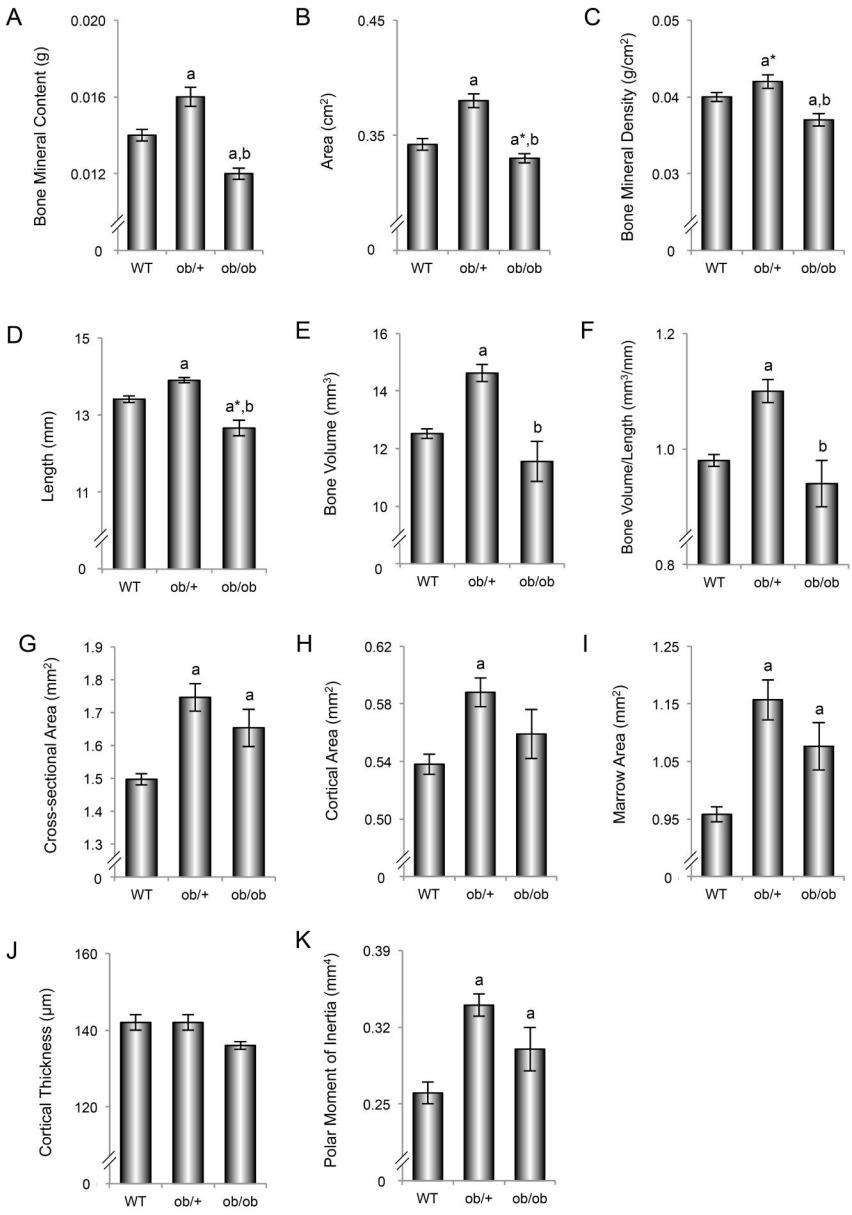

Figure 2.

Effects of genotype on femur bone mineral content (A), bone area (B), bone mineral density (C), length (D), total bone volume (E), total bone volume to length ratio (F), mid-diaphysis cross-sectional area (G), cortical area (H), marrow area (I), cortical thickness (J), and polar moment of inertia (K) in 7-week-old female WT, *ob/+*, and *ob/ob* mice. Data are mean ± SE. [a]Different from WT, $P < 0.05$; [a]*Different from WT, $P < 0.1$; [b]Different from *ob/+*, $P < 0.05$.

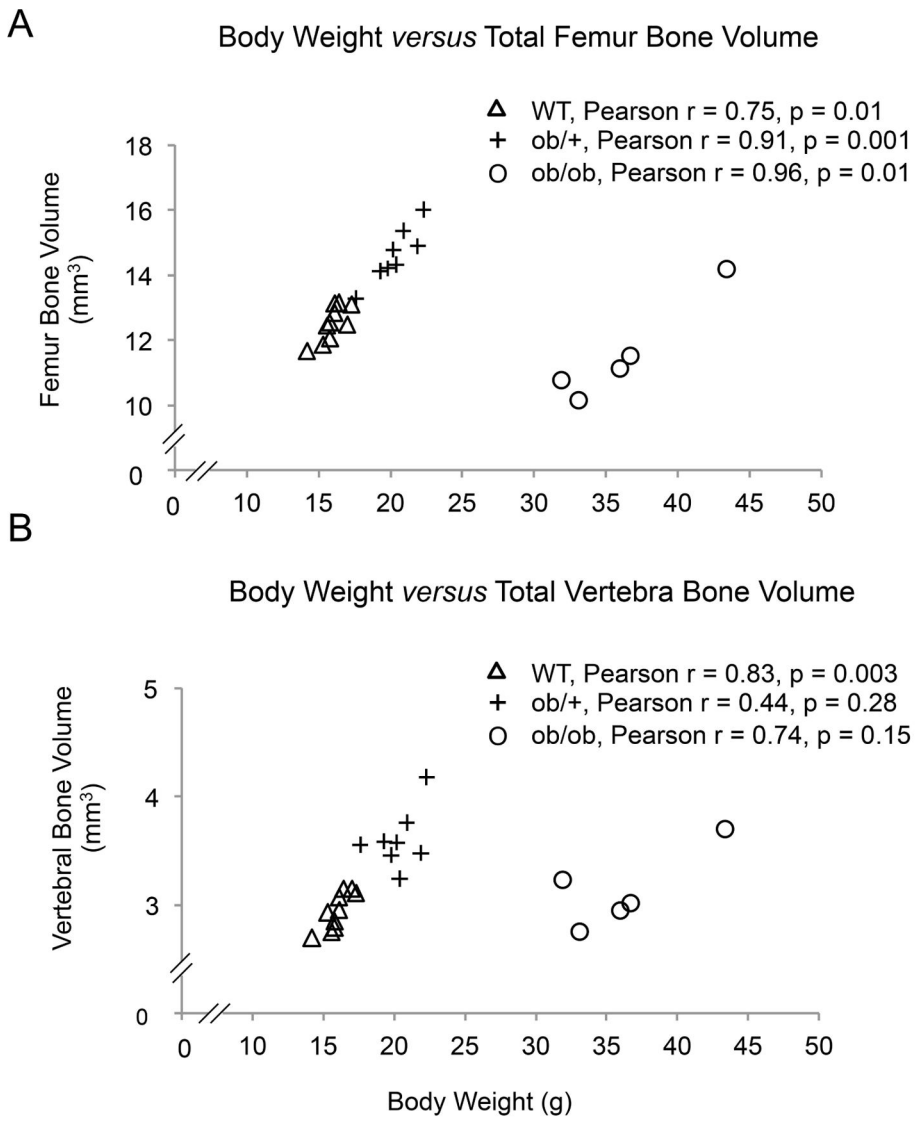

Figure 3.

Correlation between body weight and total femur bone volume (A) and body weight and total vertebra bone volume (B) in 7-week-old WT, *ob/+*, and *ob/ob* mice.

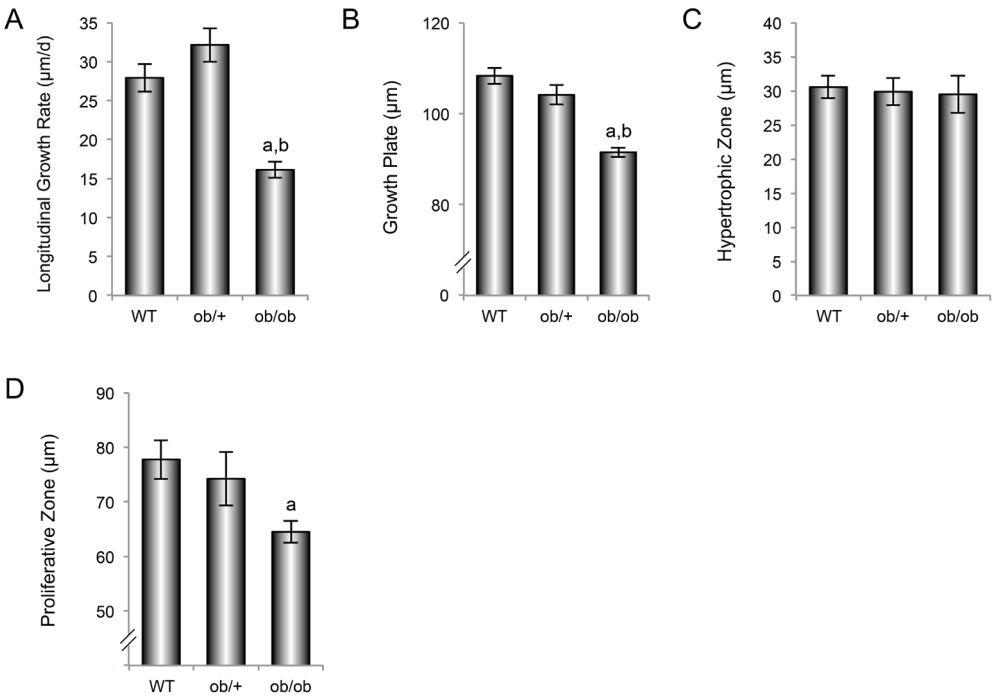

Figure 4.

Effects of genotype on distal femur longitudinal growth rate (A), growth plate thickness (B), hypertrophic zone thickness (C), and proliferative zone thickness (D) in 7-week-old female WT, *ob/+*, and *ob/ob* mice. Data are mean ± SE. [a]Different from WT, $P < 0.05$; [b]Different from *ob/+*, $P < 0.05$.

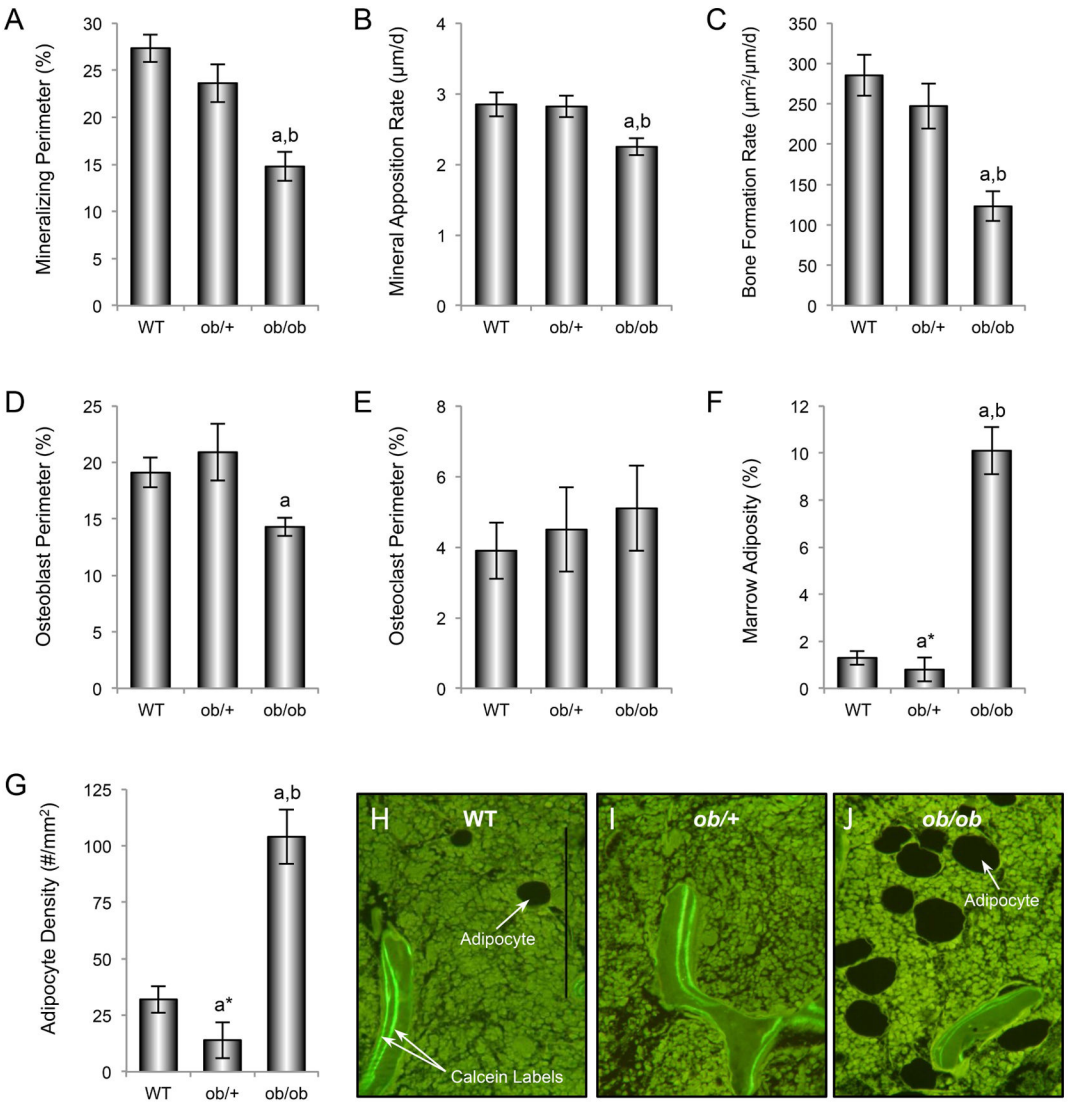

Figure 5.

Effects of genotype on distal femur metaphysis mineralizing perimeter (A), mineral apposition rate (B), bone formation rate (C), osteoblast perimeter (D), osteoclast perimeter (E), bone marrow adiposity (F), and bone marrow adipocyte density (G) in 7-week-old female WT, *ob/+*, and *ob/ob* mice. Representative histological sections illustrating differences in bone marrow adiposity and fluorochrome labeling among the 3 genotypes are shown in H-J. Data are mean ± SE. [a]Different from WT, $P < 0.05$; [b]Different from *ob/+*, $P < 0.05$. Scale bar, 200 μm.

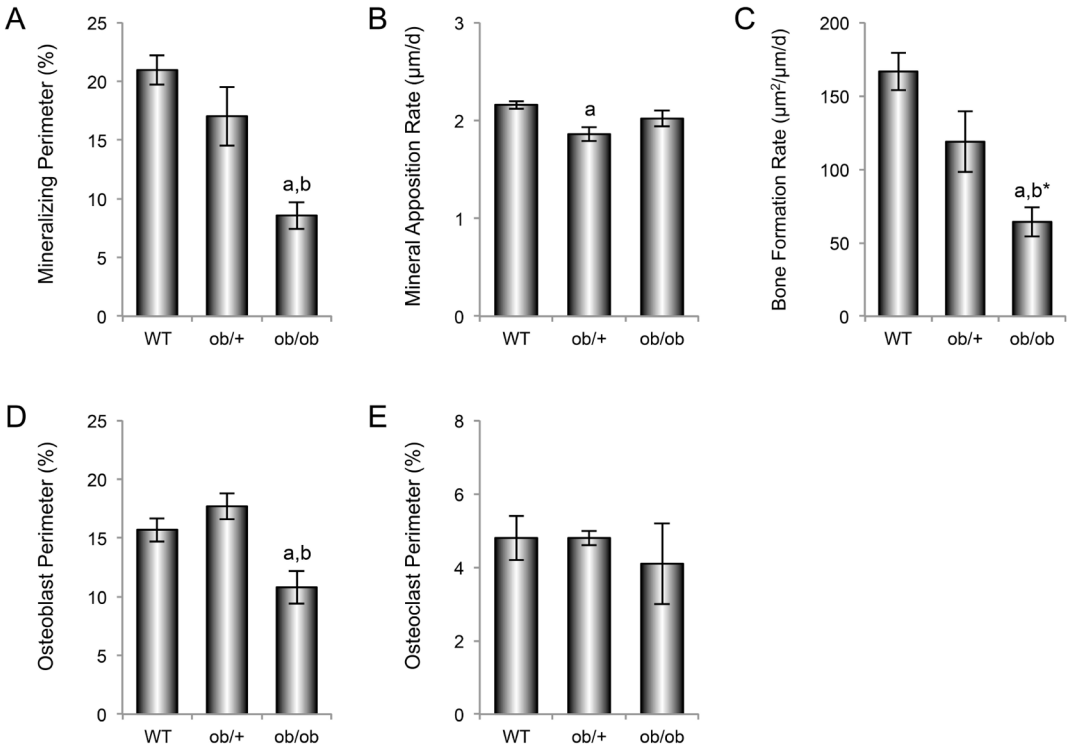

Figure 6.

Effects of genotype on vertebral mineralizing perimeter (A), mineral apposition rate (B), bone formation rate (C), osteoblast perimeter (D) and osteoclast perimeter (E) in 7-week-old WT, *ob/+*, and *ob/ob* mice. Data are mean ± SE. [a]Different from WT, $P < 0.05$; [b]Different from *ob/+*, $P < 0.05$; [b]*Different from *ob/+*, $P < 0.1$.

Table 1

Effect of genotype on cancellous bone volume fraction (bone volume/tissue volume) and cancellous bone architecture in distal femur metaphysis and epiphysis.

	WT	*ob/+*	*ob/ob*	ANOVA P[C]
Femur Metaphysis (cancellous bone)				
Bone volume/tissue volume (%)	12.5 ± 0.9	10.3 ± 0.7[a*]	8.4 ± 1[a]	0.028
Connectivity density (mm^{-3})	164 ± 12	134 ± 14	107 ± 19[a]	0.066
Trabecular number (mm^{-1})	5.7 ± 0.1	5.3 ± 0.2	4.8 ± 0.3[a]	0.050
Trabecular thickness (μm)	40 ± 1	39 ± 1	37 ± 1	0.231
Trabecular spacing (μm)	175 ± 3	192 ± 9	215 ± 14[a*]	0.066
Femur Epiphysis (cancellous bone)				
Bone volume/tissue volume (%)	25.8 ± 0.4	25.5 ± 0.6	23.8 ± 1.4	0.195
Connectivity density (mm^{-3})	286 ± 9	269 ± 7	369 ± 2[a,b]	0.000
Trabecular number (mm^{-1})	6.4 ± 0.1	6.0 ± 0.1[a]	7.1 ± 0.3[a,b]	0.001
Trabecular thickness (μm)	49 ± 1	50 ± 1	43 ± 1[a,b]	0.001
Trabecular spacing (μm)	156 ± 2	167 ± 3[a]	140 ± 7[a,b]	0.001

Data are mean ± SE

[c] The Benjamini and Hochberg method for maintaining the false discovery rate at 5% was used to adjust for multiple comparisons

[a] Different from WT, $P < 0.05$,

[a*] Different from WT, $P < 0.1$;

[b] Different from *ob/+*, $P < 0.05$

Table 2

Effect of genotype on lumbar vertebral bone volume and on cancellous bone volume fraction (bone volume/tissue volume) and cancellous bone architecture in vertebral body.

	WT	*ob/+*	*ob/ob*	ANOVA P[C]
Total Vertebra				
Bone volume (mm^3)	2.9 ± 0.1	3.6 ± 0.1[a]	3.1 ± 0.2[b]	0.001
Vertebral Body (cancellous bone)				
Bone volume/tissue volume (%)	15.6 ± 0.4	15.2 ± 0.8	18.2 ± 0.7[a,b]	0.018
Connectivity density (mm^{-3})	252 ± 9	249 ± 13	354 ± 11[a,b]	0.000
Trabecular number (mm^{-1})	5.3 ± 0.1	5.2 ± 0.1	5.9 ± 0.2[a,b]	0.001
Trabecular thickness (μm)	38 ± 0	39 ± 1	38 ± 1	0.333
Trabecular spacing (μm)	186 ± 2	191 ± 3	167 ± 5[a,b]	0.002

Data are mean ± SE

[c]The Benjamini and Hochberg method for maintaining the false discovery rate at 5% was used to adjust for multiple comparisons

[a]Different from WT, $P < 0.05$;

[b]Different from *ob*/+, $P < 0.05$